Time-Dependent, Three-Dimensional Simulation of Free-Electron-Laser Oscillators

P. J. M. van der Slot,[1] H. P. Freund,[2] W. H. Miner Jr.,[2] S. V. Benson,[3] M. Shinn,[3] and K.-J. Boller[1]

[1]*University of Twente, LPNO, MESA+ Institute for Nanotechnology, P.O. Box 217, 7500 AE Enschede, The Netherlands*

[2]*Science Applications International Corporation, McLean, Virginia 22102, USA*

[3]*Thomas Jefferson National Accelerator Facility, Newport News, Virginia 23606, USA*

(Received 2 March 2009; published 18 June 2009)

We describe a procedure for the simulation of free-electron-laser (FEL) oscillators. The simulation uses a combination of the MEDUSA simulation code for the FEL interaction and the OPC code to model the resonator. The simulations are compared with recent observations of the oscillator at the Thomas Jefferson National Accelerator Facility and are in substantial agreement with the experiment.

DOI: 10.1103/PhysRevLett.102.244802 PACS numbers: 41.60.Cr

Free-electron laser (FEL) oscillators have been demonstrated at wavelengths across the electromagnetic spectrum from the infrared through the ultraviolet [1–6]. Recently, the 10-kW upgrade experiment at the Thomas Jefferson National Accelerator Facility (henceforth referred to as Jefferson Laboratory) [1] obtained an output power of 14.3 kW. To further advance the development of high power FEL oscillators a proper simulation tool is required that can account for complex resonator configurations and the FEL gain medium including both three-dimensional and time-dependent effects in the wiggler. In this Letter, we describe such a formulation using the MEDUSA code to model the FEL interaction and OPC (optics propagation code) to model the resonator, as well as a comparison of the simulation with the 10-kW upgrade experiment at Jefferson Laboratory.

MEDUSA is a three-dimensional simulation code that includes time dependence, harmonics, and startup from noise [7–10]. It models helical and planar wigglers and the optical field is represented as a superposition of Gaussian modes. Electron trajectories are integrated using the three-dimensional Lorentz force equations in the combined magnetostatic and optical fields. No wiggler average orbit analysis is used. Models for quadrupoles and dipoles are included. The time dependence is treated in either of two ways. First, the electron beam and the optical mode are described by an ensemble of temporal slices where each slice is advanced from $z \rightarrow z + \Delta z$ as in steady-state simulations, after which the field is allowed to slip relative to the electrons. Second, an explicit polychromatic expansion of the fields can be employed. These two algorithms are equivalent [11]; however, the former is simpler to employ and is used here. Note that the first time-dependence algorithm can be combined with a polychromatic harmonic representation to treat the evolution of the fundamental and harmonics in the time domain.

OPC propagates the optical field using either the Fresnel diffraction integral or the spectral method in the paraxial approximation [12,13] using fast discrete Fourier transforms (FFT). A modified Fresnel diffraction integral [14,15] is also available and allows the use of FFTs in combination with an expanding grid on which the optical field is defined. This method is often used when diffraction of the optical beam is large. Currently, OPC includes mirrors, lenses, phase masks, and round and rectangular diaphragms. Several optical elements can be combined to form more complex optical component, e.g., by combining a mirror with a hole element, extraction of radiation from a resonator through a hole in one of the mirrors can be modeled. Phase masks can be used to model mirror distortions or to create nonstandard optical components like a cylindrical lens.

In a typical resonator configuration, OPC handles the propagation from the end of the gain medium to the first optical element, applies the action of the optical element to the optical field, and propagates it to the next optical element until it reaches the entrance of the gain medium. Diagnostics can be performed at the planes where the optical field is evaluated. Some optical elements, specifically diaphragms and mirrors allow forking of the optical path. For example, the reflected beam of a partial transmitting output mirror forms the main intracavity optical path, while the transmitted beam is extracted from the resonator. When the intracavity propagation has reached the output mirror, this optical propagation can be temporarily suspended, and the extracted beam can be propagated to a diagnostic point for evaluation. Then the intracavity propagation (main path) is resumed.

Currently, OPC interfaces with two FEL gain models, MEDUSA and GENESIS 1.3 [12,13]. Typically, the simulation of an FEL oscillator starts with one of the two gain models, in this case with MEDUSA, that will initialize the optical field and propagate it together with the electron beam through the wiggler. Then at the position of the wiggler exit, the optical field, i.e., the complex phase front, is handed over to OPC to propagate it through the down stream mirror, which in the current example is partially reflecting. The portion of the optical mode that is reflected

is then propagated to the upstream mirror (which is a high reflector) by OPC, and then back to the wiggler entrance where the optical field is handed back to the gain model. In the case of MEDUSA, the complex phase front is reduced to an ensemble of Gaussian modes that are used as input for the next pass. OPC is capable of setting parameters for the gain model that depends on the round-trip.

The numerical procedure involves translating between the input or output required for MEDUSA and OPC. Initially, we run MEDUSA to determine the optical output after the first pass through the wiggler, which then writes a file describing the complex phase front of the optical mode. OPC is then used to propagate this field to the downstream mirror, which is partially transmissive in the current example. The portion of the optical mode that is reflected is then propagated to the upstream mirror (which is a high reflector) by OPC, and then back to the wiggler entrance. The field at the wiggler entrance is then reduced to an ensemble of Gaussian modes that is used as input to MEDUSA for the next pass. This process is repeated for an arbitrary number of passes.

The experimental configuration is described in detail in Ref. [1]. The specific parameters to be used for the comparison are as follows. The electron beam has a kinetic energy of 115 MeV, a bunch charge of up to 115 pC, an energy spread of 0.3%, a pulse length of 390 fsec, and a pulse repetition frequency of 74.85 MHz. The normalized emittance is 9 mm-mrad in the wiggle plane and 7 mm-mrad in the plane normal to the wiggle plane. The beam is matched to the optical mode, so that it is focused to a spot near the center of the wiggler. The planar wiggler is 30 periods in length, has a peak on-axis amplitude of 3.75 kG, and a period of 5.5 cm. The FEL is tuned to a wavelength of 1.6 μm and the resonator is approximately 32 m long. For the experiments under consideration here, the Rayleigh range is 0.75 m. The downstream mirror is partially transmissive, and out-couples about 21% of the energy per pass.

The optimal cavity length is found in simulation to be 32.041 708 5 m, and we plot the evolution of the circulating energy in each pulse and the average output power versus pass in Fig. 1. An equilibrium state is achieved after about 40 passes with a circulating pulse energy of about 0.8 mJ. Since 21% of the pulse energy is out-coupled per pass at a repetition rate of 74.85 MHz, this translates into an average output power of 12.3 kW. An output power of 14.3 $\pm$ 0.72 kW was observed in the experiment, so that the simulation result is only approximately 9% lower than the experimental observation.

The optical pulse interacts with a fresh electron bunch on each pass, and the electron bunch is assumed to have a symmetric parabolic shape. However, due to slippage within the wiggler and different synchronism conditions between the optical pulse and the electron bunch due to the cavity tuning, the optical pulse is distorted relative to the electron bunch. This is shown in Fig. 2 where we plot the

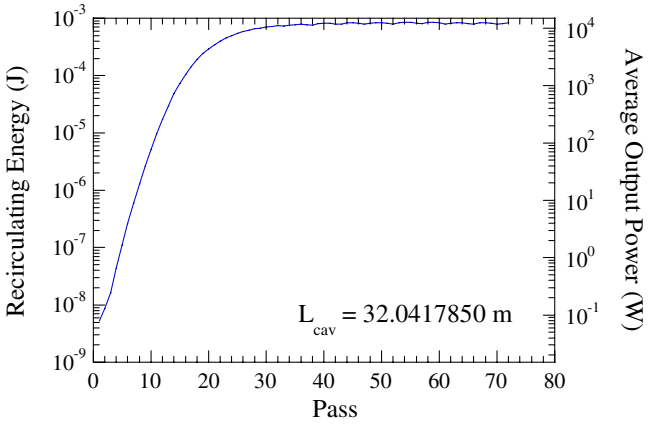

FIG. 1 (color online). Output energy and power for the optimal cavity length without aberrations.

power versus time of the optical pulse in the steady state for the optimal cavity length. Note that within the context of the limits on the time axis, the electron bunch would be centered at 0.75 psec. As a result, the optical pulse has slipped ahead of the electron bunch by about 90 fsec, which is comparable to the slippage time in the wiggler. The pulse shape is also distorted and exhibits a sharp dropoff at the head of the pulse and a more gradual rise from the tail.

The cavity tuning curve found in simulation is shown in Fig. 3, where we plot the peak recirculating power and the average output power versus the difference between a specific cavity length and the optimal cavity length. The dots in the figure denote each simulation run and the line is a least squares fit to the points. The triangle is the experimental result with an error bar of $\pm$5%. The FWHM extent of the tuning curve is about 12–13 μm, which is in good agreement with the observed tuning in the experiment. In addition, we observe that the tuning curve exhibits a roughly triangular shape in contrast to the more usually

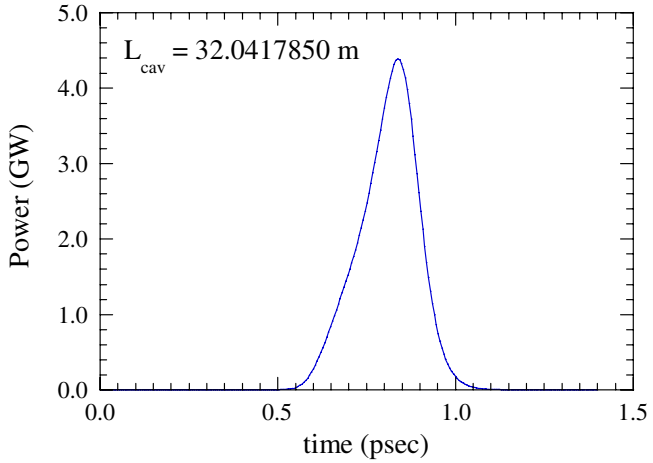

FIG. 2 (color online). Power in the output pulse versus time in the steady state.

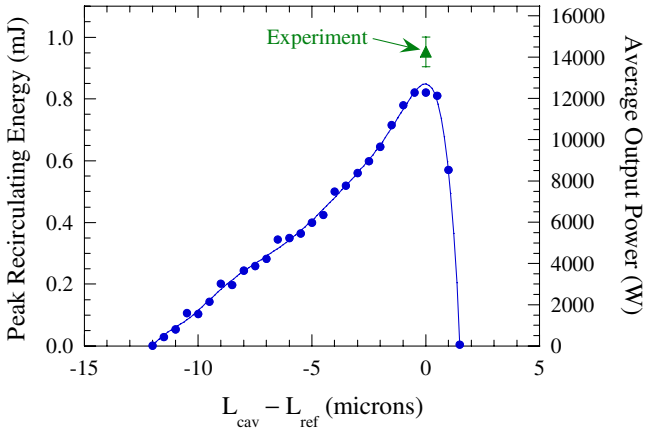

FIG. 3 (color online). Cavity tuning curve.

observed sharply peaked behavior. This is due to the relatively large outcoupling and is also observed in the experiment.

The mode sizes found in simulation on the downstream and upstream mirrors versus pass are shown in Figs. 4 and 5, respectively. The average rms mode size on both mirrors in the steady state is approximately 10–11 mm, and this is in good agreement with observations. The fluctuation occurs on a period of about 5 passes and has a magnitude of about $\pm 15\%$. At the present time, there is no unambiguous diagnostic to either confirm or refute this behavior. We note that there is a corresponding oscillation in the output power (which is difficult to observe on the logarithmic scale in Fig. 1) of about $\pm 3\%$, which is 180° out of phase with the oscillations in the mode size.

The optical mode quality observed in the experiment is near diffraction limited, and similar results are found in simulation. No quantitative diagnostic for the M^2 of the output radiation is presently implemented in the MEDUSA and OPC formulation. It should be noted that M^2 has no real

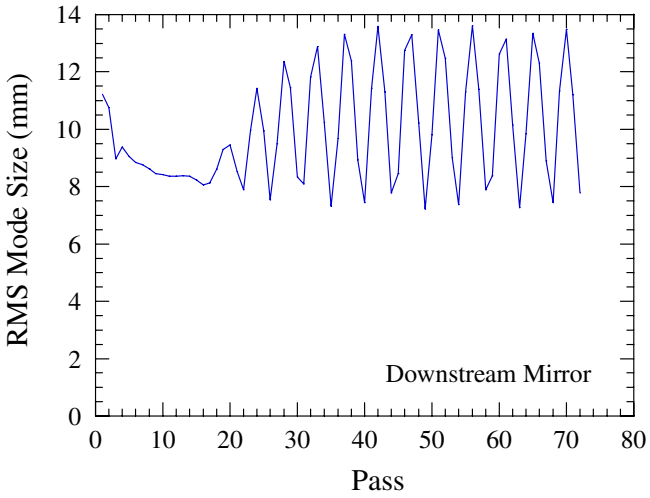

FIG. 4 (color online). Variation in the rms mode size on the downstream mirror versus pass.

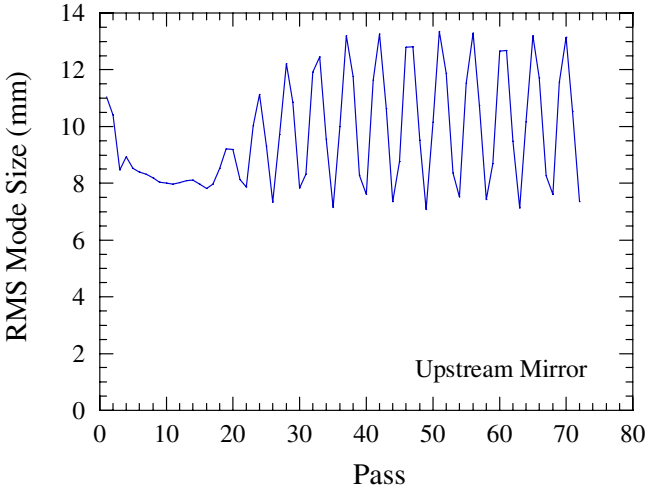

FIG. 5 (color online). Variation in the rms mode size on the upstream mirror versus pass.

meaning inside the optical resonator; however, it is possible to propagate the optical mode outside the resonator and determine the value of M^2 for the output radiation. The optical mode pattern for the optimal cavity length at the wiggler exit is shown in Fig. 6 corresponding to the peak of the pulse in steady state. The mode radius is about 1 mm and the shape is a nearly perfect Gaussian exhibiting a low higher order mode content. As indicated in Figs. 4 and 5, the mode expands as it propagates to the downstream mirror, and the mode pattern at the downstream mirror is shown in Fig. 7 with a mode radius of 10–15 mm as expected.

In summary, we have described the first comparison between the MEDUSA and OPC simulation procedure for

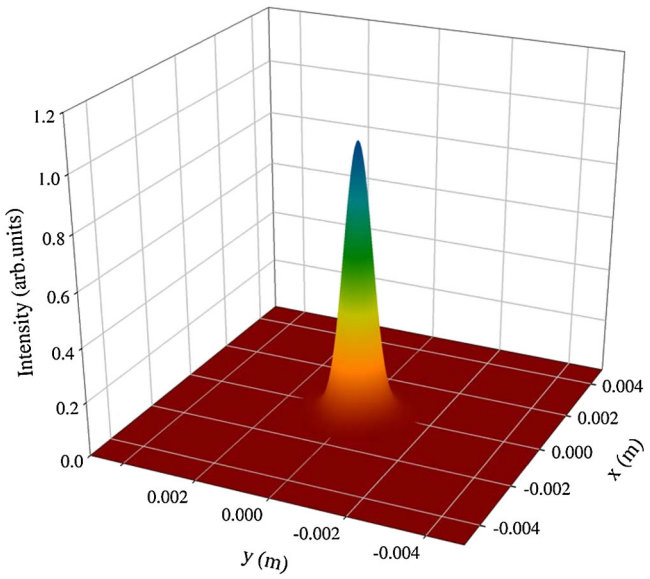

FIG. 6 (color online). Optical mode at the wiggler exit corresponding to the peak in the output pulse.

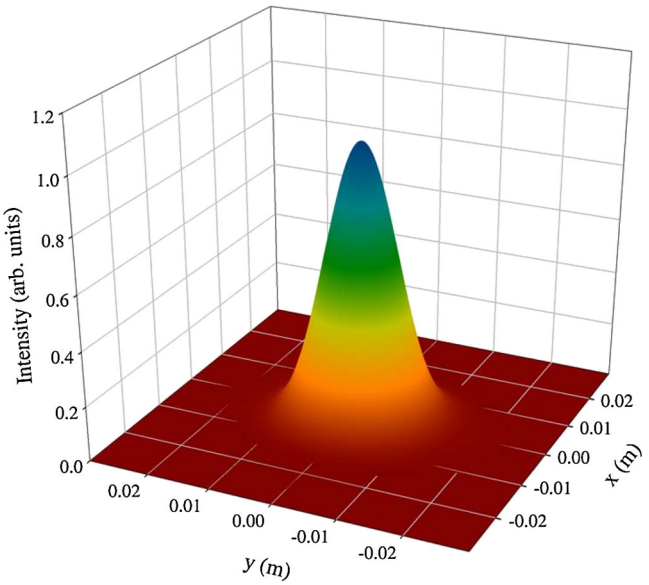

FIG. 7 (color online). Optical mode at the downstream mirror corresponding to the peak in the optical pulse.

FEL oscillators and the 10-kW upgrade experiment at Jefferson Laboratory experiment, and demonstrated good agreement between the simulation and the experiment. We remark that while MEDUSA can also include harmonics in the wiggler, OPC does not have this capability at the present time. However, the addition of this capability in OPC will be implemented in the near future.

This work represents the first validation runs for MEDUSA and OPC, and it is a forerunner to the inclusion of additional features of OPC in the simulation of FEL oscillators. For example, we now have the ability (1) to access accurate intracavity field distributions that are difficult to obtain experimentally, (2) to employ different outcoupling techniques (hole, transmissive, edge) and easily determine detuning curves, mode profiles, and efficiencies, (3) to study the effects of mirror misalignment and distortion, and (4) to simulate different resonator configurations. Finally, the simulation points the way to the necessity of new diagnostics that may be required.

This work was supported in part by the Joint Technology Office in the U.S. The authors would like to thank J. G. Karssenberg for his contribution to the OPC package.

[1] G. Neil *et al.*, Nucl. Instrum. Methods Phys. Res., Sect. A **557**, 9 (2006).
[2] P. W. van Amersfoort *et al.*, Nucl. Instrum. Methods Phys. Res., Sect. A **318**, 42 (1992).
[3] V. N. Litvinenko *et al.*, Nucl. Instrum. Methods Phys. Res., Sect. A **358**, 334 (1995).
[4] D. C. Nguyen *et al.*, Nucl. Instrum. Methods Phys. Res., Sect. A **429**, 125 (1999).
[5] N. G. Gavrilov *et al.*, Nucl. Instrum. Methods Phys. Res., Sect. A **575**, 54 (2007).
[6] R. Hajima *et al.*, Nucl. Instrum. Methods Phys. Res., Sect. A **507**, 115 (2003).
[7] H. P. Freund, Phys. Rev. A **27**, 1977 (1983).
[8] H. P. Freund *et al.*, IEEE J. Quantum Electron. **36**, 275 (2000).
[9] H. P. Freund, Phys. Rev. ST Accel. Beams **8**, 110701 (2005).
[10] H. P. Freund *et al.*, J. Appl. Phys. **104**, 123114 (2008).
[11] N. Piovella, Phys. Plasmas **6**, 3358 (1999).
[12] J. G. Karssenberg *et al.*, J. Appl. Phys. **100**, 093106 (2006).
[13] http://lpno.tnw.utwente.nl/opc.html.
[14] A. Siegman, *Lasers* (University Science Books, Mill Valley, CA, 1986).
[15] M. Born and E. Wolf, *Principles of Optics* (Pergamon Press, Oxford, 1984).